

Contributions of conserved serine and tyrosine residues to catalysis, ligand binding, and cofactor processing in the active site of tyrosine ammonia lyase

Amy C. Schroeder¹, Sangaralingam Kumaran¹, Leslie M. Hicks, Rebecca E. Cahoon, Coralie Halls, Oliver Yu, Joseph M. Jez*

The Donald Danforth Plant Science Center, 975 N. Warson Road, St. Louis, MO 63132, USA

Received 20 September 2007; received in revised form 17 December 2007

Available online 17 March 2008

Abstract

Tyrosine ammonia lyase (TAL) catalyzes the conversion of L-tyrosine to *p*-coumaric acid using a 3,5-dihydro-5-methylidene-4H-imidazole-4-one (MIO) prosthetic group. In bacteria, TAL is used for production of the photoactive yellow protein chromophore and for caffeic acid biosynthesis in certain actinomycetes. Here we biochemically examine wild-type and mutant forms of TAL from *Rhodobacter sphaeroides* (RsTAL). Kinetic analysis of RsTAL shows that the enzyme displays a 90-fold preference for L-tyrosine versus L-phenylalanine as a substrate. The pH-dependence of TAL activity with L-tyrosine and L-phenylalanine demonstrates a common protonation state for catalysis, but indicates a difference in charge-state for binding of either amino acid. Site-directed mutagenesis demonstrates that Ser150, Tyr60, and Tyr300 are essential for catalysis. Mutation of Ser150 to an alanine abrogates formation of the MIO prosthetic group, as shown by mass spectrometry, and prevents catalysis. The Y60F and Y300F mutants were inactive with both amino acid substrates, but bound *p*-coumaric and cinnamic acids with less than 12-fold changes in affinity compared the wild-type enzyme. Analysis of MIO-dithiothreitol adduct formation shows that the reactivity of the prosthetic group is not significantly altered by mutation of either Tyr60 or Tyr300. The mechanistic roles of Ser150, Tyr60, and Tyr300 are discussed in relation to the three-dimensional structure of RsTAL and related MIO-containing enzymes.

© 2008 Elsevier Ltd. All rights reserved.

Keywords: Enzyme mechanism; Prosthetic group; Mass spectrometry; Fluorescence spectroscopy; Tyrosine ammonia lyase

Tyrosine ammonia lyase (TAL) is a member of the amino acid ammonia lyase enzyme family, which also includes histidine ammonia lyase (HAL) and phenylalanine ammonia lyase (PAL). They catalyze the conversion of α -amino acids to α,β -unsaturated acids by elimination of

ammonia from tyrosine **3** (Fig. 1), histidine, and phenylalanine **1** (Fig. 1), respectively (Poppe and Rétey, 2005). These enzymes are found in plants, bacteria, and fungi. In plants, PAL catalyzes the non-oxidative deamination of L-phenylalanine **1** to *trans*-cinnamic acid **2** (Fig. 1A). This reaction is the first step in the phenylpropanoid pathway and ultimately leads to multiple classes of phenolic natural products, such as lignins, flavonoids, and isoflavonoids (Winkel-Shirley, 2001). PAL is found in dicot and monocot plants, but a secondary TAL activity is associated with the enzyme from monocots (Guerra et al., 1985; Rosler et al., 1997; Khan et al., 2003).

TAL catalyzes the conversion of L-tyrosine **3** to *p*-coumaric acid **4** (Fig. 1A). Although bacteria do not synthesize

Abbreviations: DTT, D/L-dithiothreitol; HAL, histidine ammonia lyase; IPTG, isopropyl-1-thio- β -D-galactopyranoside; MES, 2-(*N*-morpholino)ethanesulfonic acid; MIO, 3,5-dihydro-5-methylidene-4H-imidazole-4-one; NTA, nitriloacetic acid; PAL, phenylalanine ammonia lyase; RsTAL, *Rhodobacter sphaeroides* tyrosine ammonia lyase; TAL, tyrosine ammonia lyase.

* Corresponding author. Tel.: +1 314 587 1450; fax: +1 314 587 1550.

E-mail address: jjez@danforthcenter.org (J.M. Jez).

¹ Both of these authors contributed equally to the work.

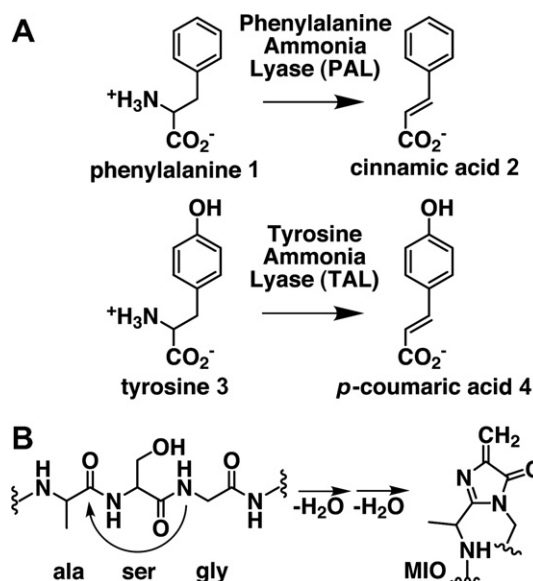


Fig. 1. Reactions catalyzed by TAL and PAL: (A) TAL generates *p*-coumaric acid **4** from L-tyrosine **3**. PAL catalyzes the conversion of L-phenylalanine **1** to cinnamic acid **2**. (B) Formation of the 3,5-dihydro-5-methylidene-4H-imidazole-4-one (MIO) prosthetic group in the TAL active site.

phenylpropanoids, PAL and TAL provide cinnamic acid **2** and *p*-coumaric acid **4**, respectively, in specialized metabolic pathways. For example, PAL is used in the biosynthesis of the marine natural product enterocin (Xiang and Moore, 2002, 2005). TAL plays a critical role in synthesizing the chromophore of photoactive yellow protein in bacteria and for caffeic acid biosynthesis in actinomycetes (Kyndt et al., 2002, 2003; Berner et al., 2006). Multiple research groups have used TAL for metabolic engineering of flavonoid and resveratrol biosynthesis pathways that require *p*-coumaric acid **4** as a precursor molecule (Watts et al., 2004; Jiang et al., 2005; Zhang et al., 2006; Qi et al., 2007; Trotman et al., 2007). Because TAL forms *p*-coumaric acid directly from L-tyrosine **3**, its use in heterologous expression systems circumvents the need to express both PAL and 4-coumaric acid hydroxylase, a membrane-bound cytochrome P450 enzyme, for conversion of L-phenylalanine **1** to *p*-coumaric acid **4**.

Historically, the amino acid ammonia-lyases were thought to use a prosthetic dehydroalanine as an electrophile in the reaction mechanism, but the three-dimensional structures of HAL and PAL indicated that these enzymes contain a 3,5-dihydro-5-methylidene-4H-imidazole-4-one (MIO) group for substrate activation (Fig. 1B) (Schwede et al., 1999; Calabrese et al., 2004; Ritter and Schulz, 2004). Spontaneous cyclization and dehydration of an alanine-serine-glycine segment of the polypeptide backbone in the active site of HAL and PAL results in formation of the MIO group (Fig. 1B) (Poppe, 2001; Baedeker and Schulz, 2002a,b; Rétey, 2003). Mechanistically, two possible reaction sequences for HAL and PAL have been proposed. The first mechanism involves direct nucleophilic addition

of the substrate α -amino group to the methylidene carbon of the MIO prosthetic group (Hermes et al., 1985). Alternatively, the reaction could occur by a Friedel–Crafts acylation mechanism in which attack of the electron-rich aromatic ring of the substrate occurs on the electron-deficient methylidene carbon of the MIO (Poppe and Rétey, 2005; Schuster and Rétey, 1995). Mutagenesis studies of HAL and PAL have probed the contribution of active site residues to catalysis (Röther et al., 2001, 2002), but a similar analysis of TAL has not been described.

Recent structural and functional studies of TAL identified a histidine in the active site as essential for controlling substrate preference for L-tyrosine **3** over L-phenylalanine **1** (Watts et al., 2006; Louie et al., 2006). Importantly, the X-ray structure of TAL gave the first view of an amino acid ammonia lyase in complex with either a reaction product or substrate analog (Louie et al., 2006). The structure shows that the MIO prosthetic group of TAL is formed from Ser150, and that a number of amino acids, including Tyr60 and Tyr300, may contribute to binding of substrates and products (Louie et al., 2006). Tyrosines corresponding to Tyr60 and Tyr300 of TAL are conserved in PAL and HAL, and each of these residues has been proposed to function as a general base in the deamination reactions catalyzed by HAL, PAL, and TAL (Schwede et al., 1999; Ritter and Schulz, 2004; Röther et al., 2001, 2002; Louie et al., 2006). The functional roles of Ser150, Tyr60, and Tyr300 in the TAL active site are the focus of this study.

1. Results

1.1. Expression, purification, and mutagenesis

The TAL gene from *Rhodobacter sphaeroides* encodes a 523 amino acid protein ($M_r = 55042.6$ Da; $pI = 7.3$), which shares 28.4%, 31.2%, and 35.6% amino acid sequence identity with *Rhodospiridium toruloides* PAL, *Petroselinum hortense* (parsley) PAL, and *Pseudomonas putida* HAL (Zhang et al., 2006). BLAST searching of sequence databases identify HAL, not PAL, as a closer relative of TAL. Hexahistidine-tagged RsTAL was purified from *E. coli* using Ni^{2+} -affinity and size-exclusion chromatographies. SDS-PAGE analysis (not shown) showed that the purified protein migrated as a 55 kDa species, as expected based on the calculated molecular weight.

To examine the contribution of selected conserved active site residues to the reaction catalyzed by RsTAL, we generated site-directed mutants of the enzyme. Based on sequence comparisons of RsTAL with PAL and HAL, we mutated Ser150 (S150A) to disrupt formation of the MIO group in the active site, Tyr300 (Y300F) to examine the contribution of this residue as a general base in the reaction mechanism, and Tyr60 (Y60F) to probe the role of a flexible active site loop (Schwede et al., 1999; Ritter and Schulz, 2004; Röther et al., 2001, 2002; Louie et al., 2006). Each RsTAL mutant was expressed and purified

with procedures used for wild-type enzyme. The final yield of soluble protein for each mutant was comparable to that obtained with wild-type RsTAL. The Y60F, S150A, and Y300F mutants behaved the same as RsTAL in SDS-PAGE and gel-filtration chromatography (not shown).

1.2. Functional analysis of wild-type RsTAL

To determine if purified recombinant RsTAL was active using aromatic amino acid substrates, the enzyme-catalyzed conversion of L-tyrosine **3** to *p*-coumaric acid **4** was monitored spectrophotometrically. Purified RsTAL was found to be active under standard assay conditions with a specific activity of 85 nmol min⁻¹ mg protein⁻¹. We also examined the ability of RsTAL to catalyze the transformation of substrate analogues, including histidine, phenylalanine, 3-iodotyrosine, and nitrophenylalanine. Of these, enzymatic activity was only observed with phenylalanine **1** (specific activity: 15 nmol min⁻¹ mg protein⁻¹). Multiple preparations of RsTAL yielded similar specific activities and steady-state kinetic parameters. The specific activity of RsTAL with tyrosine **3** as a substrate was 12-fold lower than that of the *R. capsulatus* enzyme (Kyndt et al., 2002) and 5-fold higher than that of TAL from *Saccharothrix espanaensis* (Berner et al., 2006).

Mass spectrometry verified that RsTAL produces *p*-coumaric acid **4** and cinnamic acid **2** from L-tyrosine **3** and L-phenylalanine **1**, respectively (see Section 3.5). The

steady-state kinetic parameters (k_{cat} and K_{m}) of RsTAL for tyrosine **3** and phenylalanine **1** as substrates were determined (Table 1). This analysis confirms the identity of RsTAL because comparison of the catalytic efficiencies ($k_{\text{cat}}/K_{\text{m}}$) indicates a 90-fold preference for tyrosine **3** over phenylalanine **1** as a substrate.

To obtain information about the protonation state of the reaction catalyzed by RsTAL, the pH dependence of the reaction was examined using tyrosine **1** and phenylalanine **1** as substrates (Fig. 2 and Table 2). With tyrosine **3** as a substrate (Fig. 2A), RsTAL showed pH-dependencies of k_{cat} and $k_{\text{cat}}/K_{\text{m}}$ with similar pK_a values (Table 2). Since both curves displayed similar inflection points, the enzyme–substrate complex and either free enzyme or free substrate may require deprotonation of a common chemical group for conversion of tyrosine **3** to *p*-coumaric acid **4**. In contrast, the pH-dependence of RsTAL with phenylalanine **1** as a substrate only had a breakpoint for k_{cat} with a pK_a = 6.8, and with values of $k_{\text{cat}}/K_{\text{m}}$ being independent of pH (Fig. 2B and Table 2). This suggests the loss of a binding interaction with the change in substrate, and likely reflects the loss of an interaction with the hydroxyl group of tyrosine **3**, which is not present in phenylalanine **1**.

Table 1
Steady-state kinetic parameters of RsTAL

Substrate	k_{cat} (min ⁻¹)	K_{m} (μM)	$k_{\text{cat}}/K_{\text{m}}$ (M ⁻¹ s ⁻¹)
L-tyrosine 3	4.8 ± 0.1	301 ± 48	266
L-phenylalanine 1	1.1 ± 0.1	6170 ± 740	2.97

Reactions were performed as described under Section 3. All k_{cat} and K_{m} values are expressed as a mean ± SE for an $n = 3$.

Table 2
Summary of pH-dependence of steady-state kinetic parameters

	L-tyrosine 3	L-phenylalanine 1
k_{cat} (min ⁻¹)		
pK _a	6.82 ± 0.09	6.78 ± 0.29
Y_{max}	8.29 ± 0.31	1.43 ± 0.09
$k_{\text{cat}}/K_{\text{m}}$ (M ⁻¹ s ⁻¹)		
pK _a	7.02 ± 0.17	–
Y_{max}	225 ± 20	–

Enzyme assays were performed as described under Section 3. All values are expressed as a mean ± SE for an $n = 3$. Units for the pH-independent values (Y_{max}) for each parameter are indicated.

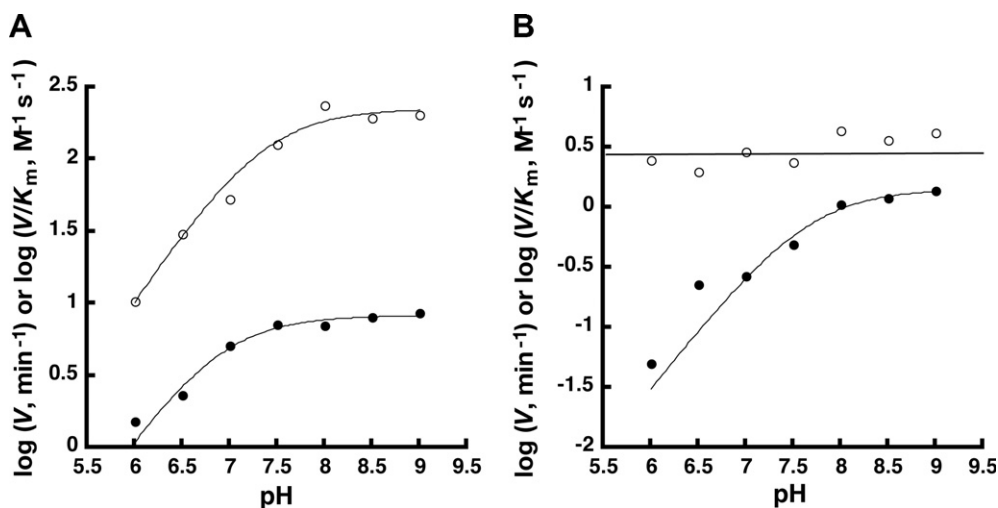


Fig. 2. pH-Dependence of steady-state kinetic parameters: (A) V (solid circles) and V/K_{m} (open circles) vs. pH profiles with L-tyrosine **3** as substrate. (B) V (solid circles) and V/K_{m} (open circles) vs. pH profiles with L-phenylalanine **1** as substrate. Lines indicate the best fit of data, as described in Section 3.

1.3. Enzymatic activity and ligand binding properties of active site mutants

For comparison with wild-type enzyme, the Y60F, S150A, and Y300F mutants were assayed for activity using L-tyrosine **3** and L-phenylalanine **1**. No reaction rates above background were observed with either substrate for any of the mutant enzymes (100 μg protein, 6 h assay length).

To determine if the active site mutations compromised ligand binding, a fluorescence titration assay was used (Fig. 3). Addition of either *p*-coumaric acid **4** or cinnamic acid **2** to RsTAL quenches the protein fluorescence emission signal (Fig. 3A). Titration of RsTAL with *p*-coumaric acid **4** and cinnamic acid **2** (Fig. 3B) yielded K_d values of 0.5 μM and 5.0 μM , respectively (Table 3). Binding of *p*-coumaric acid **4** and cinnamic acid **2** to the Y60F, S150A, and Y300F mutants using this assay showed that each mutant bound both ligands with less than 12-fold differences compared to RsTAL (Table 3). These results indicate that mutation of Tyr60, Ser150, or Tyr300 did not introduce major structural changes that drastically affect ligand binding in the active site.

1.4. Mass spectrometry analysis of the MIO cofactor

The amino acid ammonia lyases typically contain an MIO cofactor, which is formed post-translationally by cyclization of an alanine-serine-glycine segment in the active site (Fig. 1B) (Poppe, 2001; Baedeker and Schulz, 2002a,b). This consensus sequence in RsTAL includes Ala149, Ser150, and Gly151. To identify the MIO group in RsTAL, we used tryptic digestion and ESI-Q-TOF mass spectrometry. Analysis of an unfractionated trypsin digestion of RsTAL yielded a peptide species of 2159.16 Da (detected as the 3+ charge-state at m/z 720.7), correlating with the mass of the MIO-containing tryptic peptide (Gly145-Arg166) within 20 ppm (Fig. 4A). Direct fragmentation

Table 3
Analysis of product binding by fluorescence titration

	<i>p</i> -Coumaric acid 4	Cinnamic acid 2
	K_d (μM)	K_d (μM)
RsTAL	0.48 ± 0.04	5.0 ± 0.6
Y60F	2.4 ± 0.2	1.2 ± 0.4
S150A	5.8 ± 0.4	2.1 ± 0.2
Y300F	3.9 ± 0.3	1.4 ± 0.3

Fluorescence titrations were performed as described under Section 3. All K_d values are expressed as a mean \pm SE for an $n = 3$.

of this species using collisionally activated dissociation produced a series of fragment ions consistent with this peptide sequence (Fig. 4B). As shown in Fig. 4C, multiple fragment ions were assigned to the peptide, while the absence of fragmentation in the region containing Ala149-Gly151 gives further evidence for the presence of the MIO modification. Additionally, a species of 2195.16 Da was detected that correlates to the mass of the unmodified form of the tryptic peptide within 20 ppm (Fig. 4A). Fragmentation of this 3+ species at 733 m/z confirmed the identity of this peptide species (Figs. 4D & E). Fragment ions in the region between Ala149 and Gly151 are further evidence that the peptide is not modified. This suggests that the final sample contains a mixture of RsTAL containing the MIO cofactor and protein lacking the active site modification. It should be noted that the relative intensities of the two forms cannot be estimated from intensity of the ion fragments.

Analysis of the S150A mutant clearly shows that the mutation prevents formation of the MIO prosthetic group. Mass spectrometry of an unfractionated trypsin digestion of the S150A mutant yielded a peptide species of 2179.15 Da, correlating with the mass of the unmodified tryptic peptide (Gly145-Arg166) within 20 ppm (Fig. 5A). Direct fragmentation of this species using collisionally activated dissociation produced a series of fragment ions consistent with this peptide sequence (Fig. 5B). As shown in

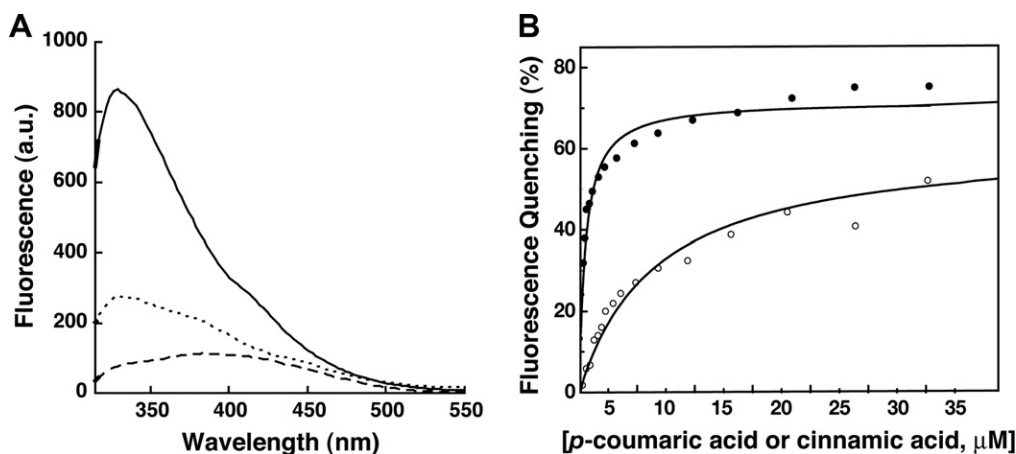


Fig. 3. Fluorescence titration analysis of product binding: (A) Emission spectra of RsTAL (1.5 μM protein) (solid line) and RsTAL in the presence of 30 μM *p*-coumaric acid **4** (dashed line) or 30 μM cinnamic acid **2** (dotted line). Excitation wavelength was 290 nm. Emission intensity is reported in a.u. = arbitrary units. (B) Titration of *p*-coumaric acid **4** (solid circles) and cinnamic acid **2** (open circles) binding to RsTAL. Data are plotted as the percentage of fluorescence change versus ligand concentration. Lines indicate the best fit of data, as described in Section 3.

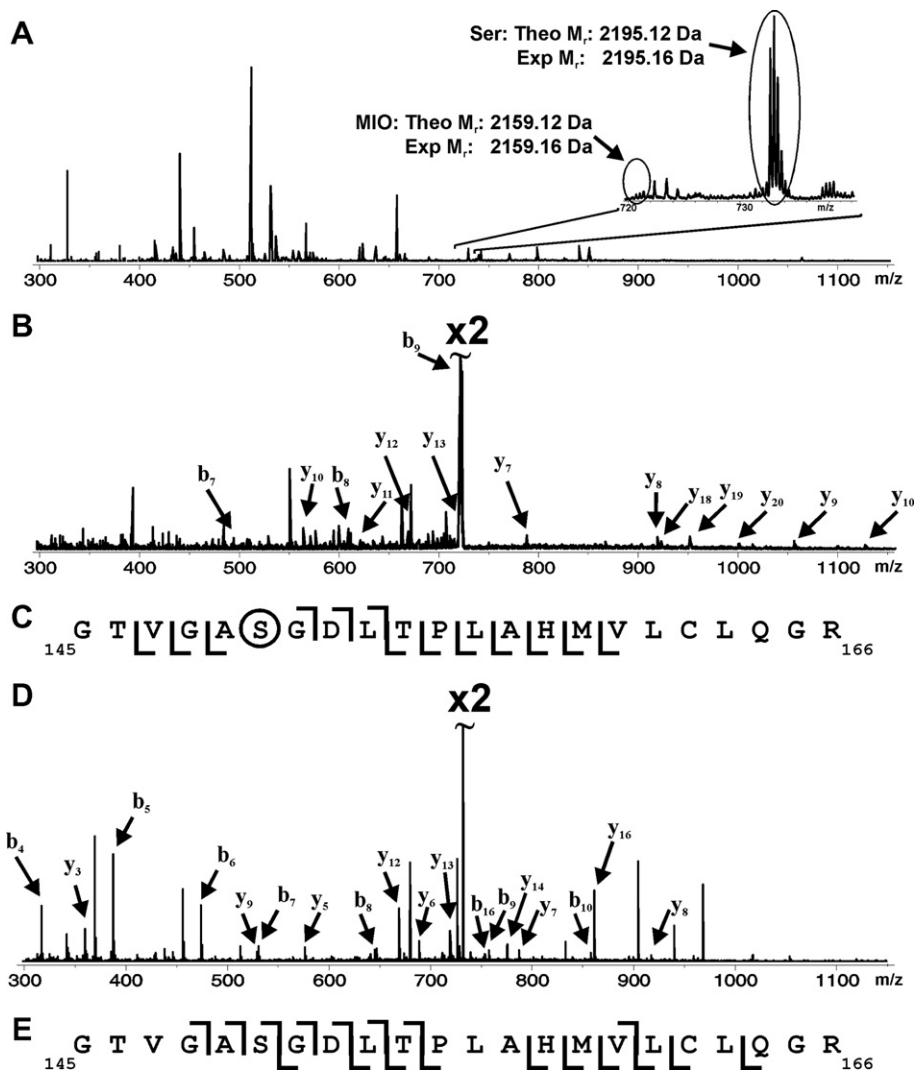


Fig. 4. Mass spectrometric analysis of wild-type RsTAL: (A) ESI-Q-TOF mass spectrum (m/z 300–1150) of an unfractionated tryptic digestion; inset (m/z 720–740) highlights the 3+ charge-state corresponding to the MIO-containing peptide of interest (theoretical M_r : 2159.12 Da) and unmodified active site peptide (theoretical M_r : 2195.12 Da). (B) MS/MS fragmentation of the 3+ charge-state (m/z 720.7). (C) Graphical fragment map correlating the fragmentation ions to the sequence of the MIO-containing peptide. The active site serine residue is circled. (D) MS/MS fragmentation of the 3+ charge-state (m/z 732.7). (E) Graphical fragment map correlating the fragmentation ions to the sequence of the unmodified active site peptide.

Fig. 5C, multiple fragment ions were assigned to the peptide predicted sequence. There was no evidence for an MIO cofactor-containing peptide, as would be indicated by a 2143.12 Da species, nor evidence of any residual Ser150 in the active site of the mutant preparation (expected 2195.12 Da species).

1.5. MIO–DTT adduct formation in wild-type and mutant RsTAL

To evaluate if mutation of either Tyr60 or Tyr300 altered the reactivity of the active site MIO group, a covalent modification assay was used. Earlier work describes the inactivation of PAL by DTT via formation of a thiol-adduct with the MIO cofactor (Ritter and Schulz, 2004). Likewise, through a similar mechanism, cysteine forms a thiol-adduct with MIO in HAL that changes the spectral

properties of the prosthetic group (Schuster and Rétey, 1995). In this experiment, we incubated wild-type and mutant TAL in the presence of various concentrations of DTT and monitored changes in fluorescence emission over time (Fig. 6). Kitz–Wilson analysis of the changes in MIO emission signal from formation of the thiol-adduct between DTT and the MIO cofactor in wild-type RsTAL showed pseudo-first order kinetics with a $k_{\text{inact}} = 0.08 \text{ h}^{-1}$ and $K_I = 14.5 \text{ mM}$ (Fig. 6, inset). Modification of wild-type RsTAL by DTT was also monitored by activity assays using L-tyrosine as a substrate and showed a loss in enzymatic activity that paralleled the loss in MIO emission signal (not shown). Although enzymatic activity could not be monitored in the mutant enzymes, modification of MIO by DTT showed changes in the fluorescence emission signals of the Y60F and Y300F mutants (Fig. 6, inset), which yielded inactivation constants similar to wild-type

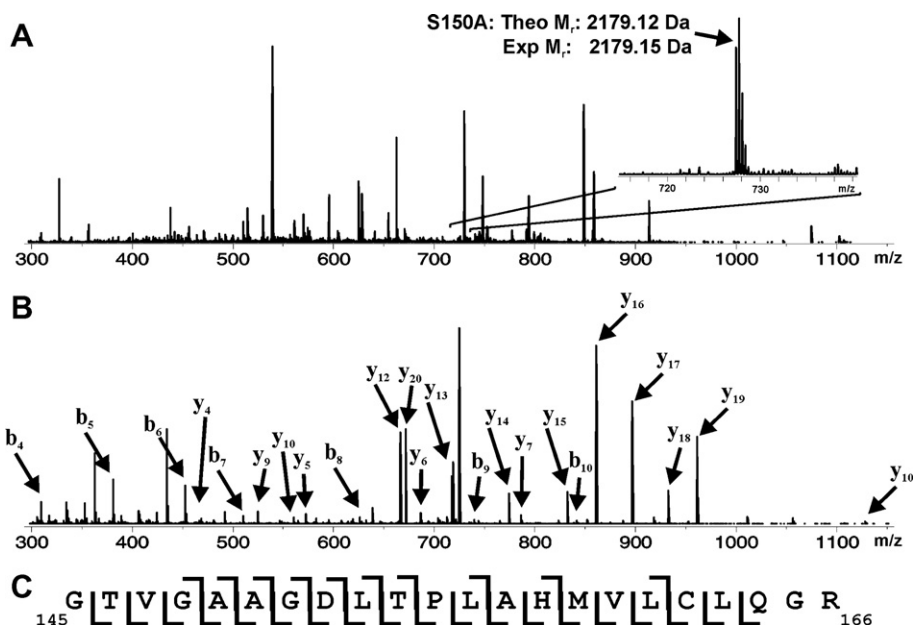


Fig. 5. Mass spectrometric analysis of the S150A mutant RsTAL. (A) ESI-Q-TOF mass spectrum (m/z 300–1150) of an unfractionated tryptic digestion; inset (m/z 715–740) highlights the 3+ charge-state corresponding to the unmodified S150A active site peptide (theoretical M_r : 2179.12 Da). (B) MS/MS fragmentation of the 3+ charge-state (m/z 727.4). (C) Graphical fragment map correlating the fragmentation ions to the sequence of the unmodified S150A active site peptide.

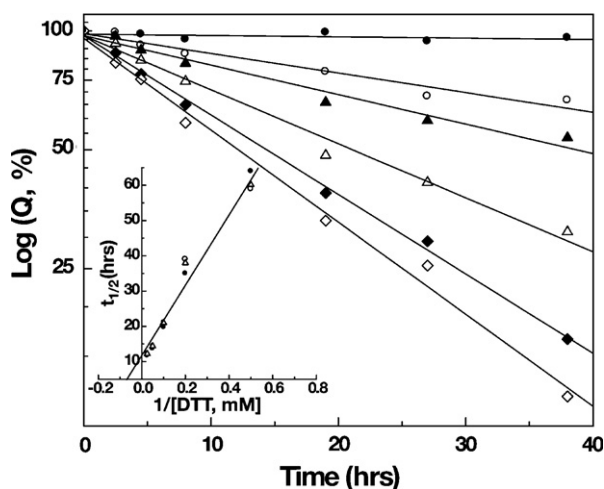


Fig. 6. Kinetics of MIO-DTT adduct formation in wild-type and mutant RsTAL. Time- and concentration-dependent modification of MIO by DTT. Wild-type RsTAL was incubated in the presence of 0, 2, 5, 10, 20, or 40 mM DTT (top to bottom) with fluorescence emission of the MIO prosthetic group monitored over time, as described in Section 3. The inset shows the Kitz-Wilson analysis of DTT modification for wild-type (solid circle), Y60F (open circle), and Y300F (open triangle) RsTAL. The line shows the fit of the wild-type data.

Table 4
DTT-modification kinetics of wild-type and mutant RsTAL

	k_{inact} (h^{-1})	K_I (μM)
RsTAL	0.08 ± 0.01	14.5 ± 0.1
Y60F	0.08 ± 0.01	10.3 ± 0.1
Y300F	0.09 ± 0.01	16.7 ± 0.1

Modification studies were performed as described under Section 3. All values were obtained by Kitz-Wilson analysis and are expressed as a mean \pm SE for an $n = 3$.

enzyme (Table 4). This suggests that the reactivity of the MIO cofactor in the wild-type and mutant enzymes are similar.

2. Discussion

TAL and other enzymes of the amino acid ammonia lyase family convert α -amino acids to α,β -unsaturated acids by elimination of ammonia (Poppe and Rétey, 2005). The X-ray structure of TAL yielded the first view of an amino acid ammonia lyase in complex with either a reaction product or substrate analog (Louie et al., 2006). As in HAL and PAL (Schwede et al., 1999; Calabrese et al., 2004; Ritter and Schulz, 2004), the active site of TAL centers around an MIO prosthetic group, which is formed by the autocatalytic cyclization of a three-amino acid loop that includes Ser150 (Poppe, 2001; Baedeker and Schulz, 2002a,b; Louie et al., 2006). Mechanistically, each of the two alternate reaction sequences proposed for the amino acid ammonia lyase family requires a general base for catalysis (Schwede et al., 1999; Calabrese et al., 2004; Ritter and Schulz, 2004; Baedeker and Schulz, 2002a,b; Louie et al., 2006). Within the active site of TAL, both Tyr60 and Tyr300 have been proposed to serve this function. Using RsTAL, we have examined the roles of Ser150, Tyr60, and Tyr300 in catalysis, ligand binding, and MIO processing.

Conversion of tyrosine 3 and phenylalanine 1 into *p*-coumaric acid 4 and cinnamic acid 2, respectively, by RsTAL occurs through a common chemical mechanism, as indicated by the similar pH-dependence of k_{cat} for the

substrates (Fig. 2A and Table 2). Removal of the substrate hydroxyl group results in a pH-independent $k_{\text{cat}}/K_{\text{m}}$ profile for phenylalanine **1** (Fig. 2B and Table 2), which suggests the loss of a binding interaction in the active site. As elegantly shown by Watts et al. (2006) and Louie et al. (2006), a histidine in the active site of TAL determines the substrate preference for tyrosine **3** over phenylalanine **1**. In the crystal structure of TAL (Louie et al., 2006), the histidine side-chain forms a hydrogen bond with the hydroxyl group of the tyrosine **3** substrate. The observed $\text{p}K_{\text{a}}$ in the $k_{\text{cat}}/K_{\text{m}}$ rate profile of TAL for tyrosine **3** likely corresponds to the active site histidine.

Site-directed mutagenesis of Ser150, Tyr60, and Tyr300 in the RsTAL active site yields mutant enzymes with no detectable activity using either tyrosine **3** or phenylalanine **1** as substrate, indicating that each of these conserved active site residues is essential for catalysis. Mutation of the residue corresponding to Tyr60 in HAL and PAL caused 2650- and 75,000-fold reductions in specific activity, respectively (Röther et al., 2001, 2002). Likewise, 55- and 235-fold decreases in reaction rate occurred with mutation of the residue corresponding to Tyr300 in HAL and PAL, respectively (Röther et al., 2001, 2002). Previous studies of HAL and PAL only report changes in reaction rates (Röther et al., 2001, 2002). Here we employed additional methods to evaluate the effect of mutating these residues on ligand binding and formation of the MIO prosthetic group. As demonstrated using fluorescence titrations, the S150A, Y60F, and Y300F mutant enzymes bind *p*-coumaric **4** and cinnamic acids **3** with modest changes in K_{d} values (Fig. 3 and Table 3), indicating that the loss of enzymatic activity upon mutation of these active site residues does not result from the inability to bind ligands.

Mutation of Ser150 in RsTAL prevents formation of the MIO prosthetic group, as shown by ESI-Q-TOF mass spectrometric analysis of wild-type and mutant enzymes (Figs. 4 and 5). Formation of the MIO moiety of TAL, HAL, and PAL occurs through the spontaneous cyclization and dehydration of an alanine-serine-glycine segment of the polypeptide backbone in the active site (Fig. 1B) (Poppe, 2001; Baedeker and Schulz, 2002a,b). This reaction is analogous to cyclization of the chromophores in green and red fluorescent proteins (Ormo et al., 1996; Wall et al., 2000). Mass spectrometry of wild-type RsTAL (Fig. 4) showed a heterogeneous mixture of the MIO-containing and unprocessed forms of the active site peptides, even though quantitation could not be surmised in this experiment. The difference in peak intensities could reflect difference in ionization efficiencies of the processed (MIO-containing) and unprocessed (no MIO) active site peptides. In addition, the cyclized MIO-containing peptide may interfere with protease digestion, as trypsin binds linear polypeptide backbones. Nonetheless, mutation of Ser150 to an alanine blocks the autocyclization reaction (Figs. 1B and 5) required for formation of the catalytic MIO group of RsTAL and results in a catalytically compromised mutant protein.

Substitutions of Tyr60 and Tyr300 with a phenylalanine **1** in the RsTAL active site yield inactive mutant enzymes that retain the ability to bind aromatic ligands. Previously, formation of MIO-thiol adducts was used to monitor the reactivity of the MIO prosthetic group in the active sites of both HAL and PAL (Schuster and Rétey, 1995; Ritter and Schulz, 2004). Here we used a fluorescence-based assay to monitor DTT adduct formation by changes in the MIO emission signal of wild-type and mutant RsTAL (Fig. 6 and Table 4). Although generation of the MIO–DTT adduct is not the optimal reaction catalyzed by the enzyme (Poppe and Rétey, 2005; Poppe, 2001), this assay indicates that mutations in Tyr60 and Tyr300 do not significantly alter the reactivity of the MIO prosthetic group.

As shown here, both Tyr60 and Tyr300 are critical for efficient catalysis in TAL; however, the contribution of either residue to the TAL reaction mechanism remains equivocal. Mechanistically, the hydroxyl group of tyrosine **3** requires activation through interactions with other active site residues to serve as a general acid/base (Blomster et al., 1995; Jornvall et al., 1995; Jez et al., 1997; Schlegel et al., 1998; Liu et al., 1999).

In the three-dimensional structure of RsTAL, Tyr300 forms a hydrogen bond with Gln436, which in turn interacts with a water molecule in the active site (Louie et al., 2006). This set of interactions may reduce the $\text{p}K_{\text{a}}$ of Tyr300 allowing it to serve as a general base. Substitution of a phenylalanine **1** for Tyr300 likely disrupts this network and affects the local active site structure. In the X-ray crystal structure of HAL containing a phenylalanine mutation at the corresponding position, differences in the active site architecture were observed (Baedeker and Schulz, 2002b). The tyrosine-to-phenylalanine mutation did not shift the position of the side-chain phenyl group, but eliminated a hydrogen bond formed with an adjacent glutamate residue (Glu414 in HAL) that results in a large displacement of the acidic side-chain into the binding site (Baedeker and Schulz, 2002b). Moreover, the nitrogen atom of the MIO prosthetic group contributed from the glycine residue changed from a pyramidal sp^3 hybridization to a planar sp^2 hybridization state (Baedeker and Schulz, 2002b). Given the similarity of TAL and HAL, analogous structural changes may alter how the substrate fits in the active site, such that the loss of activity results from altered positioning of the substrate relative to the MIO prosthetic group (without compromising binding affinity), and/or disruption of the hydrogen bond network interacting with this residue.

Alternatively, the structure of TAL (Louie et al., 2006) and mutagenesis of both HAL and PAL (Röther et al., 2001, 2002) suggest that Tyr60 could act as the general base in the reaction catalyzed by the amino acid ammonia lyases. Within the RsTAL active site, Tyr60 resides in a highly conserved flexible loop that forms an “innerlid” of the active site (Louie et al., 2006). In earlier crystallographic studies of HAL and PAL, the analogous structural regions were either disordered or displayed high

temperature factors (Schwede et al., 1999; Calabrese et al., 2004; Ritter and Schulz, 2004). Molecular dynamics simulations of PAL implied that this loop may be functionally important (Pilbak et al., 2006), but the structures of RsTAL in complex with products demonstrated for the first time that Tyr60 moves into close contact with bound *p*-coumaric acid **4** (Louie et al., 2006). The experiments described here show that removal of the hydroxyl group from this residue in the Y60F RsTAL mutant yields inactive protein that binds *p*-coumaric and cinnamic acids and retains a reactive MIO prosthetic group.

How Tyr60 is activated to function as a general base in the TAL reaction mechanism is unclear. All of the reported structures for the amino acid ammonia lyases are either for apoenzyme or product/inhibitor complexes; no view of a substrate or substrate-analog bound to the enzyme is available to show the positions of active site residues in the Michaelis complex. Interestingly, a mechanism for activation of Tyr60 to serve as a general base is suggested by recent structural studies of a related enzyme, i.e., tyrosine aminomutase. Christianson et al. (2007) used a mechanism-based inactivation strategy to obtain a crystal structure of the MIO-containing tyrosine aminomutase in complex with a substrate analog covalently attached to the MIO group. The tyrosine aminomutase active site is structurally similar to those of TAL, PAL, and HAL, and contains an MIO-prosthetic group and residues analogous to Tyr60 and Tyr300 in positions similar to RsTAL. In the tyrosine aminomutase structure, the residue corresponding to Tyr60 is positioned near the α - and β -carbons of the substrate analog in a position suggesting its function as a general base. The hydroxyl group of the tyrosine **3** interacts with the nitrogen of an adjacent glycine residue, which is conserved in TAL and other amino acid ammonia lyases. This interaction and the contribution of helical dipoles in the active site are suggested to lower the pK_a of this tyrosine. Moreover, mutation of this residue in tyrosine aminomutase yields inactive enzyme (Christianson et al., 2007).

2.1. Conclusion

In conclusion, the details of the reaction mechanism and the roles of specific active site residues in the amino acid ammonia lyase family remain contested and unresolved. Ultimately, definitive evidence for the mechanistic roles of the two active site tyrosine residues requires further structural and functional studies.

3. Experimental

3.1. Materials

Oligonucleotides were synthesized by Integrated DNA Technologies. The pET28a bacterial expression vector and the *Escherichia coli* Rosetta (DE3) cells were from

Novagen. The QuikChange PCR-based mutagenesis kit was purchased from Stratagene. Ni²⁺-nitriloacetic acid (NTA)-agarose was bought from Qiagen. The Superdex-200 26/60 FPLC column was from Amersham Biosciences. All other reagents were purchased from Sigma–Aldrich.

3.2. Bacterial expression vector construction and site-directed mutagenesis

The coding region of RsTAL was amplified by PCR from a previously described yeast expression vector (Zhang et al., 2006) using 5'-dTTTGCTAGCATGCTGCCATGA-3' as the forward primer (NdeI site is underlined; the start codon is in bold) and 5'-dTTTGGATCCTCAGAGGGGAGATTGC-3' as the reverse primer (BamHI site is underlined and the stop codon is in bold). The PCR product was subcloned into the pET28a vector to yield pET28a-RsTAL expression vector. Automated nucleotide sequencing confirmed the fidelity of the expression construct (Washington University Sequencing Facility).

The Y60F and Y300F site-directed mutants of RsTAL were generated using the QuikChange (Stratagene) PCR method with pET28a-RsTAL as template. Presence of mutations in the resulting vectors was confirmed by DNA sequencing. Due to the high GC content of the region around the codon for Ser150, an alternate strategy was used to generate the S150A RsTAL mutant. The expression construct of the RsTAL S150A mutant was generated by amplifying a 227 nucleotide region of the gene containing the mutation, which was flanked by PstI and FspI sites. Primers for the amplification of this region were 5'-dTTTCTGCAGGCCAATCTTGTCATCATCTGGC-CAGCGGC (forward primer, PstI site underlined), and 5'-dTTTTCGCAAGCGGTGTCAGGTCACCCGCGC-CCACCG (reverse primer, FspI site underlined and the mutated basepair for the serine to alanine mutation is indicated in bold italic). PCR products were amplified from the pET28a-RsTAL template using PfuTurbo polymerase (Invitrogen), digested with FspI and PstI, and ligated into FspI/PstI-digested pET28a, where conditions were adjusted to give partial digestion with FspI due to the presence of an FspI site in the vector. Automated nucleotide sequencing of both strands confirmed the fidelity of the final vector.

3.3. Protein expression and purification

Expression constructs were transformed into *E. coli* Rosetta (DE3) cells. Transformed cells were grown at 37 °C in Terrific Broth containing 50 $\mu\text{g ml}^{-1}$ kanamycin and 34 $\mu\text{g ml}^{-1}$ chloramphenicol until the $A_{600\text{ nm}}$ was 0.6–0.8. Protein expression was induced by addition of isopropyl-1-thio- β -D-galactopyranoside (IPTG) (1 mM final). Cells were grown 4–6 h at 20 °C before harvesting by centrifugation. Cell pellets were resuspended in 50 mM Tris (pH 8), 500 mM NaCl, 20 mM imidazole, 10% (v/v) glycerol, and 1% (v/v) Tween-20 and then sonicated. After

centrifugation, the supernatant was passed over a Ni^{2+} -NTA column equilibrated in the same buffer as above. After washing the column in 50 mM Tris (pH 8), 500 mM NaCl, 20 mM imidazole, and 10% (v/v) glycerol, bound protein was eluted using the same buffer containing 250 mM imidazole. To remove the *N*-terminal His-tag, thrombin was added to eluate, which was then dialyzed overnight (4 °C) against 50 mM Tris (pH 8.0), 500 mM NaCl, 20 mM imidazole, and 10% (v/v) glycerol. The sample was depleted of thrombin and uncut protein by running over a mixed benzamidine-sepharose/ Ni^{2+} -NTA column. Flow-through from this step was loaded onto a Superdex-200 26/60 size-exclusion FPLC column equilibrated in 50 mM Tris (pH 8) and 100 mM NaCl. Fractions containing RsTAL were pooled and stored at -80 °C. Protein concentrations were determined using Bradford reagent (Bio-Rad) with bovine serum albumin as standard.

3.4. Enzyme assays

Standard assays of TAL activity were performed at 25 °C in 0.5 mL volume containing 50 mM Tris (pH 8) and 2 mM *L*-tyrosine for 10 min. Production of *p*-coumaric acid **4** ($A_{310\text{ nm}}$; $\epsilon = 17,423\text{ M}^{-1}\text{ cm}^{-1}$) from *L*-tyrosine **3** was monitored using a Beckman DU800 spectrophotometer. Conversion of *L*-phenylalanine **1** to *trans*-cinnamic acid **2** ($A_{290\text{ nm}}$; $\epsilon = 10,000\text{ M}^{-1}\text{ cm}^{-1}$) was measured spectrophotometrically under similar conditions. Steady-state kinetic parameters were determined by initial velocity experiments with *L*-tyrosine **3** and *L*-phenylalanine **1**. The untransformed data were fit to the Michaelis–Menten equation using Kaleidagraph (Syngery Software). pH-rate profiles were obtained using a triple buffer system (50 mM sodium acetate, 50 mM 2-(*N*-morpholino)ethanesulfonic acid (MES), and 50 mM Tris, final concentrations) in place of Tris buffer (Ellis and Morrison, 1982). Data were fit to the equation for increasing activity vs. pH, $\log Y = \log (c/1 + H/K_a)$, where Y is the measured parameter (k_{cat} or k_{cat}/K_m), K_a is the dissociation constant for the titrated group, and c is the pH-independent value of Y (Cleland, 1979).

3.5. Product identification

Purified RsTAL (1 μg) was incubated with 2 mM *L*-tyrosine **3** or *L*-phenylalanine **1** for 20 min in 10 mM Tris (pH 8.5) at 30 °C. The reaction mixture was then extracted with EtOH_2 and separated using an LC-20AD HPLC system (Shimadzu, Tokyo, Japan) equipped with a Spherisorb ODS-2 reversed phase C-18 column (5 μm ; 250×4.6 mm). Compounds were loaded with solvent A (1% (v/v) AcOH), followed by elution with a linear gradient of solvent B (5–70% (v/v) CH_3CN) for 40 min at a flow rate of 0.5 mL min^{-1} . Product identity was first confirmed by comparison of retention time with standards. Mass spectrometric analysis used a Q-TRAP 4000 quadrupole

tandem mass spectrometer (Applied Biosystems) outfitted with an electrospray ion source. Information-dependent analysis of samples and authentic standards was operated in positive mode with the source voltage of 5.5 kV and source temperature of 500 °C. In the enhanced MS scan mode, scans were carried out between m/z 100 and 1000. In the enhanced product ion scan mode, parent ions were fragmented with collision energy +25 kV. Fragments were monitored between m/z 50 and 600. The observed m/z values of the parent ion and fragmentation pattern for each product were determined, as follows: *p*-coumaric acid, $[\text{C}_9\text{O}_3\text{H}_8+\text{H}]^+$ 165.09, $[\text{C}_9\text{O}_2\text{H}_7+\text{H}]^+$ 149.02, $[\text{C}_8\text{OH}_7+\text{H}]^+$ 121.06; cinnamic acid, $[\text{C}_9\text{O}_2\text{H}_8+\text{H}]^+$ 149.05, $[\text{C}_9\text{OH}_7+\text{H}]^+$ 132.04, $[\text{C}_8\text{H}_7+\text{H}]^+$ 104.06, which were confirmed with authentic standards.

3.6. Analysis of MIO formation by mass spectrometry

Proteolysis was performed by addition of TPCK-treated trypsin (Promega) to purified wild-type or S150A RsTAL (100 μg) at a protease to substrate ratio of 1:10 (w/w) in 50 mM NH_4HCO_3 (pH 7.8) and incubated at 30 °C for 15 min. Reactions were quenched by the addition of 20% (v/v) HCO_2H (10 μL) and subjected to C18 Zip-Tip (Millipore) purification for desalting before analysis by electrospray ionization quadrupole time-of-flight (ESI-Q-TOF) mass spectrometry. Sample analysis proceeded with an ABI QSTAR XL (Applied Biosystems/MDS Sciex) hybrid QTOF MS/MS mass spectrometer equipped with a nanoelectrospray source (Protana XYZ manipulator). Positive mode nanoelectrospray was generated from borosilicate nanoelectrospray needles at 1.5 kV. TOF mass spectra were obtained using the Analyst QS software with an m/z range of 300–2000. The m/z response of the instrument was calibrated with standards from the manufacturer. Species of interest were selected using the quadrupole and subjected to collisionally activated dissociation (MS/MS) for confirmation of peptide identification. The fragmentation data were interpreted using Analyst BioTools software and ProSight PTM for correlation of fragment ions to the peptide primary amino acid sequence.

3.7. Fluorescence titration analysis of product binding

TAL was dialyzed in 50 mM Tris (pH 8) and 150 mM NaCl. Fluorescence measurements were made on a Varian Cary fluorimeter ($\lambda_{\text{excitation}} = 295\text{ nm}$ and $\lambda_{\text{emission}} = 345\text{ nm}$; slit widths = 5 nm). Titrations were performed at 25 °C by addition of either *p*-coumaric acid or cinnamic acid to 0.5 mL of 50 mM Tris (pH 8) and 150 mM NaCl containing 1.5 μM of wild-type or mutant protein. Control titrations with buffer alone did not produce any change in emission signal. The K_d value was calculated using Kaleidagraph with the data fit to $\Delta F = (\Delta F_{\text{max}}[\text{L}])/([\text{L}] + K_d)$, where ΔF is the change in emission signal in the presence of ligand (L) and ΔF_{max} is the maximal change in signal.

3.8. Assay of MIO-modification by DTT

Wild-type or mutant RsTAL was incubated in 50 mM Tris (pH 8) and 150 mM NaCl in the presence of 0 to 40 mM D/L-dithiothreitol (DTT) at 25 °C. The change in fluorescence emission signal of the MIO prosthetic group ($\lambda_{\text{excitation}} = 310$ nm and $\lambda_{\text{emission}} = 350$ nm; slit widths = 5 nm) was monitored over time. Control incubations showed no change in the emission signal of MIO over the time range used. The resulting data was plotted as log (percent quenching of signal) versus time, which were fit to the first-order equation, $-dQ/dt = k[I]$, where the change in emission signal (Q) over time is related to the concentration of DTT, $[I]$, multiplied by k , a rate constant. Using this equation, the half-life for modification of the MIO cofactor ($t_{1/2}$) was determined for each DTT concentration. Kitz–Wilson analysis of the data yielded the limiting rate constant for inactivation (k_{inact}) and K_I (Kitz and Wilson, 1962).

Acknowledgments

This work was supported by grants from the National Science Foundation (MCB0519634), the U.S. Department of Agriculture (2005-05190), and the Missouri Soybean Merchandising Council (02-242) to O.Y. Funding for the Q-TRAP 4000 mass spectrometer was provided through a National Science Foundation grant (DBI-0521250). A.C.S. was supported by a National Science Foundation Research Experiences for Undergraduates grant (DBI-0244155) and an American Society of Plant Biologists Summer Undergraduate Research Fellowship. ProSight PTM, used by L.M.H., was developed in the laboratory of Prof. Neil Kelleher (Department of Chemistry, U. Illinois-Urbana-Champaign).

References

- Baedeker, M., Schulz, G.E., 2002a. Autocatalytic peptide cyclization during chain folding of histidine ammonia-lyase. *Structure* 10, 61–67.
- Baedeker, M., Schulz, G.E., 2002b. Structures of two histidine ammonia-lyase modifications and implications for the catalytic mechanism. *Eur. J. Biochem.* 269, 1790–1797.
- Berner, M., Krug, D., Bihlmaier, C., Vente, A., Muller, R., Bechthold, A., 2006. Genes and enzymes involved in caffeic acid biosynthesis in the actinomycete *Saccharothrix espanaensis*. *J. Bacteriol.* 188, 2666–2673.
- Blomster, M., Wetterholm, A., Mueller, M.J., Haeggstrom, J.Z., 1995. Evidence for a catalytic role of tyrosine 383 in the peptidase reaction of leukotriene A4 hydrolase. *Eur. J. Biochem.* 231, 528–534.
- Calabrese, J.C., Jordan, D.B., Boodhoo, A., Sariaslani, S., Vannelli, T., 2004. Crystal structure of phenylalanine ammonia lyase: multiple helix dipoles implicated in catalysis. *Biochemistry* 43, 11403–11416.
- Christianson, C.V., Montavon, T.J., Festin, G.M., Cooke, H.A., Shen, B., Bruner, S.D., 2007. The mechanism of MIO-based aminomutases in β -amino acid biosynthesis. *J. Am. Chem. Soc.* 129, 15744–15745.
- Cleland, W.W., 1979. Statistical analysis of enzyme kinetic data. *Methods Enzymol.* 63, 103–138.
- Ellis, K.J., Morrison, J.F., 1982. Buffers of constant ionic strength for studying pH-dependent processes. *Methods Enzymol.* 87, 405–426.
- Guerra, D., Anderson, A.J., Salisbury, F.B., 1985. Reduced phenylalanine ammonia-lyase and tyrosine ammonia-lyase activities and lignin synthesis in wheat grown under low pressure sodium lamps. *Plant Physiol.* 78, 126–130.
- Hermes, J.D., Weiss, P.M., Cleland, W.W., 1985. Use of nitrogen-15 and deuterium isotope effects to determine the chemical mechanism of phenylalanine ammonia-lyase. *Biochemistry* 24, 2959–2967.
- Jez, J.M., Bennett, M.J., Schlegel, B.P., Lewis, M., Penning, T.M., 1997. Comparative anatomy of the aldo-keto reductase superfamily. *Biochem. J.* 326, 625–636.
- Jiang, H., Wood, K.V., Morgan, J.A., 2005. Metabolic engineering of the phenylpropanoid pathway in *Saccharomyces cerevisiae*. *Appl. Environ. Microbiol.* 71, 2962–2969.
- Jornvall, H., Persson, M., Krook, M., Atrian, S., Gonzalez-Duarte, R., Jeffrey, J., Ghosh, D., 1995. Short-chain dehydrogenases/reductases. *Biochemistry* 34, 6003–6013.
- Khan, W., Prithiviraj, B., Smith, D.L., 2003. Chitosan and chitin oligomers increase phenylalanine ammonia-lyase and tyrosine ammonia-lyase activities in soybean leaves. *J. Plant Physiol.* 160, 859–863.
- Kitz, R., Wilson, I.B., 1962. Acceleration of the rate of reaction of methanesulfonyl fluoride and acetylcholinesterase by substituted ammonium ions. *J. Biol. Chem.* 237, 3235–3239.
- Kyndt, J.A., Meyer, T.E., Cusanovich, M.A., Van Beeumen, J.J., 2002. Characterization of a bacterial tyrosine ammonia lyase, a biosynthetic enzyme for the photoactive yellow protein. *FEBS Lett.* 512, 240–244.
- Kyndt, J.A., Vanrobaeys, F., Fitch, J.C., Devreese, B.V., Meyer, T.E., Cusanovich, M.A., Van Beeumen, J.J., 2003. Heterologous production of *Halorhodospira halophila* holo-photoactive yellow protein through tandem expression of the postulated biosynthetic genes. *Biochemistry* 42, 965–970.
- Liu, Y., Barrett, J.E., Schultz, P.G., Santi, D.V., 1999. Tyrosine 146 of thymidylate synthase assists proton abstraction from the 5-position of 2'-deoxyuridine 5'-monophosphate. *Biochemistry* 38, 848–852.
- Louie, G.V., Bowman, M.E., Moffitt, M.C., Baiga, T.J., Moore, B.S., Noel, J.P., 2006. Structural determinants and modulation of substrate specificity in phenylalanine-tyrosine ammonia-lyases. *Chem. Biol.* 13, 1327–1338.
- Ormo, M., Cubitt, A.B., Kallio, K., Gross, L.A., Tsien, T.Y., Remington, S.J., 1996. Crystal structure of the *Aequorea victoria* green fluorescent protein. *Science* 273, 1392–1395.
- Pilbak, S., Tomin, A., Rétey, J., Poppe, L., 2006. The essential tyrosine-containing loop conformation and the role of the C-terminal multi-helix region in eukaryotic phenylalanine ammonia-lyases. *FEBS J.* 273, 1004–1019.
- Poppe, L., 2001. Methylidene-imidazolone: a novel electrophile for substrate activation. *Curr. Opin. Chem. Biol.* 5, 512–524.
- Poppe, L., Rétey, J., 2005. Friedel–Crafts-type mechanism for the enzymatic elimination of ammonia from histidine and phenylalanine. *Angew. Chem. Int. Ed.* 44, 3668–3688.
- Qi, W.W., Vannelli, T., Breinig, S., Ben-Bassat, A., Gatenby, A.A., Haynie, S.L., Sariaslani, F.S., 2007. Functional expression of prokaryotic and eukaryotic genes in *Escherichia coli* for conversion of glucose to *p*-hydroxystyrene. *Metab. Eng.* 9, 268–276.
- Rétey, J., 2003. Discovery and role of methylidene imidazolone, a highly electrophilic prosthetic group. *Biochim. Biophys. Acta* 1647, 179–184.
- Ritter, H., Schulz, G.E., 2004. Structural basis for the entrance into the phenylpropanoid metabolism catalyzed by phenylalanine ammonia-lyase. *Plant Cell* 16, 3426–3436.
- Rosler, J., Krekel, F., Amrhein, N., Schmid, J., 1997. Maize phenylalanine ammonia-lyase has tyrosine ammonia-lyase activity. *Plant Physiol.* 113, 175–179.
- Röther, D., Poppe, L., Viergutz, S., Langer, B., Rétey, J., 2001. Characterization of the active site of histidine ammonia-lyase from *Pseudomonas putida*. *Eur. J. Biochem.* 268, 6011–6019.

- Röther, D., Poppe, L., Morlock, G., Viergutz, S., Rétey, J., 2002. An active site homology model of phenylalanine ammonia-lyase from *Petroselinum crispum*. *Eur. J. Biochem.* 269, 3065–3075.
- Schlegel, B.P., Jez, J.M., Penning, T.M., 1998. Mutagenesis of 3 α -hydroxysteroid dehydrogenase reveals a “push–pull” mechanism for proton transfer in aldo-keto reductases. *Biochemistry* 37, 3538–3548.
- Schuster, B., Rétey, J., 1995. The mechanism of action of phenylalanine ammonia-lyase: the role of prosthetic dehydroalanine. *Proc. Natl. Acad. Sci. USA* 92, 8433–8437.
- Schwede, T.F., Rétey, J., Schulz, G.E., 1999. Crystal structure of histidine ammonia-lyase revealing a novel polypeptide modification as the catalytic electrophile. *Biochemistry* 38, 5355–5361.
- Trotman, R.J., Camp, C.E., Ben-Bassat, A., Dicosimo, R., Huang, L., Crum, G.A., Sariaslani, F.S., Haynie, S.L., 2007. Calcium alginate bead immobilization of cells containing tyrosine ammonia lyase activity for use in the production of *p*-hydroxycinnamic acid. *Biotechnol. Prog.* 23, 638–644.
- Wall, M.A., Socolich, M., Ranganathan, R., 2000. The structural basis for red fluorescence in the tetrameric GFP homolog DsRed. *Nature Struct. Biol.* 7, 1133–1138.
- Watts, K.T., Lee, P.C., Schmidt-Dannert, C., 2004. Exploring recombinant flavonoid biosynthesis in metabolically engineered *Escherichia coli*. *ChemBiochem* 5, 500–507.
- Watts, K.T., Mijts, B.N., Lee, P.C., Manning, A.J., Schmidt-Dannert, C., 2006. Discovery of a substrate selectivity switch in tyrosine ammonia-lyase, a member of the aromatic amino acid lyase family. *Chem. Biol.* 13, 1317–1326.
- Winkel-Shirley, B., 2001. Flavonoid biosynthesis. A colorful model for genetics, biochemistry, cell biology, and biotechnology. *Plant Physiol.* 126, 485–493.
- Xiang, L., Moore, B.S., 2002. Inactivation, complementation, and heterologous expression of encP, a novel bacterial phenylalanine ammonia-lyase gene. *J. Biol. Chem.* 277, 32505–32509.
- Xiang, L., Moore, B.S., 2005. Biochemical characterization of a prokaryotic phenylalanine ammonia lyase. *J. Bacteriol.* 187, 4286–4289.
- Zhang, Y., Li, S.Z., Pan, X., Cahoon, R.E., Jaworski, J.G., Wang, X., Jez, J.M., Chen, F., Yu, O., 2006. Using unnatural protein fusions to engineer resveratrol biosynthesis in yeast and mammalian cells. *J. Am. Chem. Soc.* 128, 13030–13031.